

Learning Disentangled Representation for Ising Model

Dongchen Huang,^{1,2} Danqing Hu,^{1,2} and Yi-feng Yang^{1,2,3,*}

¹*Beijing National Laboratory for Condensed Matter Physics and Institute of Physics,
Chinese Academy of Sciences, Beijing 100190, China*

²*University of Chinese Academy of Sciences, Beijing 100049, China*

³*Songshan Lake Materials Laboratory, Dongguan, Guangdong 523808, China*

Finding disentangled representation plays a predominant role in the success of modern deep learning applications, but the results lack a straightforward explanation. Here we apply the information bottleneck method to find as an example the disentangled low-dimensional representation of the Ising model. Our results reveal a deep connection between the disentangled features and the physical order parameters of the model. The widely-used Bernoulli decoder is found to be learning a mean-field Hamiltonian at fixed temperature, which motivates us to propose a modified architecture β^2 -VAE to enforce thermal fluctuations in the learned samples under generation. Our framework may be extended to other more complex models to reveal potential connection between their order parameters and disentangled low-dimensional representations.

I. INTRODUCTION

Representation learning lies in the core of modern deep learning. With given tasks such as in supervised learning, deep learning methods have achieved unprecedented success in computer vision [1–3] and deep reinforcement learning [4–6]. However, it is still very challenging to establish clear criteria for the learned representations [3, 7]. In practice, algorithmic designs are guided by some *meta-priors* on general premises about the relevant domain knowledge [8]. One of the most popular and typical meta-priors is *disentanglement*, which in a recent line of works [8–11] has been argued to be a good characteristic of representations. A key intuition of disentanglement is that a good representation requires the data to have some independent generative factors that are explainable and semantically meaningful and have the ability of reconstruction, which is also the goal of generative modeling. Two typical methods are often used for the generative model. One is the likelihood-free method which parameterizes the probability distribution directly with deep neural network [12, 13]. The other is the likelihood-based method [9, 11, 14, 15], which assumes an explicit probability distribution of the input data.

The most prevalent likelihood-based methods are restrictive Boltzmann machines (RBMs) and variational autoencoders (VAEs). RBMs [16] and their quantum extensions [17] have many applications in the field of many-body physics [18–22] and quantum information [23–25], such as approximating wave functions [26], performing quantum state tomography [24], and learning the Ising model even near criticality [27]. By contrast, VAEs are relatively less applied in physics, although they have been extensively explored in machine learning. VAEs have the advantage of learning the latent representation and the probability distribution of the input data simultaneously [14, 15], which is lacking in RBMs due to the difficulty in interpreting the latent representations and generating high-fidelity images. VAEs can also well capture the

physical properties with the usage of convolutional layers [28] and make further predictions [29]. Their linear versions, namely the principal component analysis (PCA) and its kernel extension [30], have been shown to be a useful extractor to identify phase transitions [31]. It is therefore interesting to explore more applications of VAEs in physics.

On the other hand, combining prior knowledge into learning algorithms also plays a crucial role in designing neural network [32–37]. In physics, people also look for simplified representation of the complex world. The interaction of physics and representation learning may lead to potential improvement of both fields. The exploration of VAEs in physics may potentially improve the expressive power and interpretability. In fact, previous machine learning applications have mostly focused on studying *raw* data rather than controlling latent representations. It is natural to ask what is the disentangled representation for the *physical* data as reflected in the latent space, and to what extent the learned representation resembles the true physical knowledge.

To simplify the discussions, here we make the attempt to address these questions by studying the classical Ising model as an example. We apply the state-of-the-art disentanglement learning method β -VAE to approximate the *sufficient statistic* of configuration samples of the Ising model and show that introducing an extra hyperparameter can simultaneously improve the quality of both representation and reconstruction. This leads to better interpretability of the disentangled representation and projects different physical properties onto different axes of the latent space. We further find that the popular Bernoulli decoder can be viewed as a mean-field solver for an effective local Hamiltonian, providing a physical interpretation of the last layer of the decoder. This motivates us to propose a novel physics-informed algorithm that can yield learned features in potential correspondence with real physical properties. We also show that the distance in input space is protected with a well-trained

encoder via maximum mean discrepancy [38].

II. METHOD

We first introduce the β -VAE method recently developed based on the information bottleneck principle. The latter provides a candidate criteria for good representations and has the advantage to be approximately implemented within the framework of generative modelling.

A. Information bottleneck

A good representation must satisfy both sufficiency and simplicity. The condition of sufficiency can be realized by introducing the so-called *sufficient statistic*. For a given random variable X with the probability distribution $P(X)$, its sufficient statistic is a random variable Z that contains all the information of X in the sense that $I(Z; X) = H(X)$, where $H(X)$ is the Shannon entropy of X and $I(Z; X)$ is the *mutual information* between Z and X defined by

$$I(Z; X) = \sum_{Z, X} P(Z, X) \log \frac{P(Z, X)}{P(Z)P(X)}. \quad (1)$$

Here $P(Z, X)$ is the joint probability of Z and X . We have $I(Z; X) = 0$ if and only if X and Z are independent. Thus the mutual information may also be used to illustrate the correlation between a pair of random variables.

The condition of simplicity is, however, less obvious. A common empirical assumption is disentanglement, where high dimensional observations can be described by a hidden low dimensional set of independent factors. Recently, it has been shown that in order to achieve disentanglement, it is necessary to not only make the common factorization assumption of random variables in the latent space, but also introduce explicit inductive biases referring to task [7]. The latter means to introduce another random variable Y so that the optimal representation Z may ignore some irrelevant information of X but encode the most relevant information with respect to Y . In this case, there may exist other sufficient statistic that contains more information of X but has a more involved form than Z .

Obviously, the choice of representation Z is not unique. Information bottleneck principle [39, 40] aims to find the approximate simplest (minimal) sufficient statistic. It can be shown that Z satisfies the constrained optimization problem:

$$Z = \underset{\substack{S(X); \\ I(S(X); X) \leq I_c}}{\operatorname{argmax}} I(S(X); Y), \quad (2)$$

where Y is the given task (e.g. classification), I_c controls how much information is to be ignored, and $S(X)$ is a

transformation of the random variable X . If the mutual information of Z and X equals the Shannon entropy of X , the optimal representation is also sufficient statistic by definition. For Gaussian distribution of X , the sufficient statistic is simple and well-known, *i.e.*, its mean and variance. But in general, it is an intractable task to obtain the exact formulation of optimal sufficient statistic. An approximate may be computed under the framework of the information bottleneck principle by computing

$$Z = \underset{Z}{\operatorname{argmax}} [I(Z; Y) - \beta I(Z; X)], \quad (3)$$

where the Lagrange multiplier β controls the relevance of Z with respect to X . This links closely to the generative modelling where the task Y is nothing but the intrinsic probability distribution of the data and the random variable X obeys the empirical distribution of the samples. Thus, in the following, we will not distinguish the random variables X and Y . The meta-prior of disentanglement appears in the assumption of the structure of the latent variable Z , where high dimensional observations can be described by a hidden low dimensional set of independent factors.

B. β -VAE

The above information bottleneck framework can be directly implemented through generative models, but the mutual information I is notoriously hard to estimate exactly. The problem is then approximated to minimize the loss function [41],

$$\begin{aligned} \mathcal{L} = & - \int p_D(x) q_\phi(z|x) \log p_\theta(x|z) dx dz \\ & + \beta \frac{1}{N} \sum_{i=1}^N D_{\text{KL}}[q_\phi(z|x_i) \| p(z)], \end{aligned} \quad (4)$$

where $p_D(x)$ is the true data distribution, $q_\phi(z|x)$ is the posterior probability distribution approximated by the encoder neural network, $p_\theta(x|z)$ is the parameterized data distribution implemented by the Bernoulli decoder for binary variable, x_i denotes a sample from the dataset, N is the size of the dataset, $p(z)$ is the prior distribution of the latent variable often chosen to be Gaussian, and D_{KL} is the so-called Kullback-Leibler (KL) divergence,

$$D_{\text{KL}}[f(z) \| g(z)] = \int dz f(z) \log f(z)/g(z). \quad (5)$$

The posterior $q_\phi(z|x)$ is chosen to be Gaussian to enable the usage of reparameterization trick to avoid high gradient variance [14]. For $\beta = 1$, the above formula recovers the so-called evidence lower bound (ELBO) used in VAEs [14, 15]. The first term refers to the log-likelihood of the data and its value reflects the distortion of the

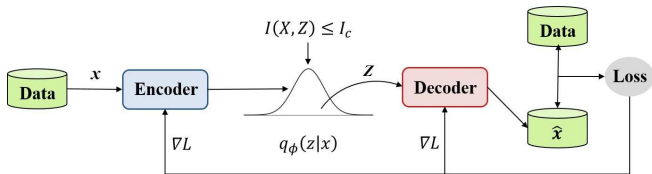


FIG. 1: An overview of β -VAE within the encoder-decoder framework. The encoder maps the input sample x into the latent space subject to the mutual information constraint. The resulting latent sample z satisfies the posterior distribution $q_\phi(z|x)$ usually chosen to be a disentangled multivariate Gaussian in a much lower dimension. The decoder is trained to map the latent space back to the original input space and generate a decoded sample \hat{x} which is typically “slimier” or close to the input sample x .

reconstruction. The second term gives the distance of the output $q_\phi(z|x_i)$ and the prior distribution $p(z)$, and its value is zero when no information is encoded. New samples can be generated by running the decoder alone after training. Different choices of the hyperparameter β control the trade-off between exact reconstruction (first term) and the extraction of information (second term). The algorithms are hence called β -VAE [11], where one may choose a proper value of β to obtain the best disentangled representation z . An overview of the β -VAE is shown in Fig. 1.

III. APPLICATION TO THE ISING MODEL

We apply the above framework to the classical Ising model on a square lattice,

$$H = -J \sum_{\langle ij \rangle} S_i S_j + h \sum_i S_i, \quad (6)$$

where $S_i = \pm 1$ is the Ising spin, J is the exchange coupling, and h is the magnetic field. The sum over $\langle ij \rangle$ denotes that only the nearest neighbor interaction is considered. For $h = 0$, the model undergoes a ferromagnetic (FM) or antiferromagnetic (AFM) phase transition at the critical temperature $T_c/|J| \approx 2.269$ depending on the sign of J [42]. For simplicity, we set $|J| = 1$ as the energy unit and generate the data set of size 100000 via Monte Carlo simulations on the square lattice of the size $L = 32$. The algorithm is implemented with Tensorflow [43] using the Adam optimizer [44], as elaborated in the Appendix. For better visualization, we set the dimension of the latent variable z to 2. We will train the network on the whole dataset including paramagnetic (PM) samples and discuss the quality of their generated samples and the latent representations with respect to the value of β . For convenience, we will set $h = 0$ and use binary data $\sigma_i \in \{0, 1\}$ to represent the up/down configuration of the Ising spins.

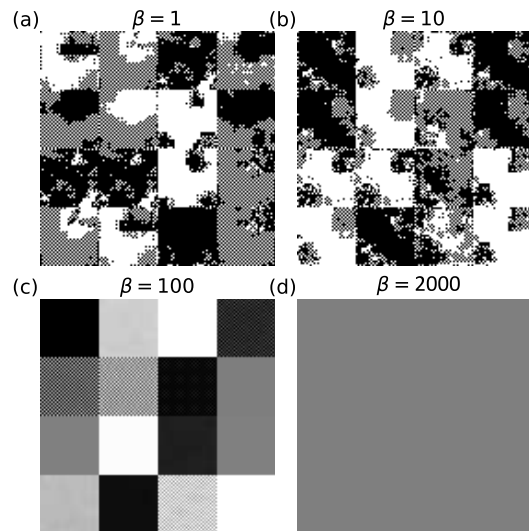


FIG. 2: Comparison of typical generated samples for the hyperparameter $\beta = 1, 10, 100, 2000$ in three-phase learning. Each small square represents a spin configuration on the $L \times L$ lattice and each panel contains 16 samples. The white, black, gray pixels reflect the learned m_k of roughly 0, 1, 1/2. Hence, the white and black regions correspond to FM phases of opposite polarization, the gray region is PM, and the checkered region is AFM. Only at $\beta = 100$, all three phases are well reproduced and separated. At small β , the PM phase is ignored, while at large β , the FM and AFM phases are missing.

Figure 2 compares the generated data for different choices of β . Each small square corresponds to one sampled spin configuration on the $L \times L$ lattice and each panel contains 16 independent samples. Their different patterns correspond to the FM (black and white), AFM (checkered), and PM (gray) phases, respectively. Only for $\beta = 100$, the trained model can correctly generate samples for all three phases, while for usual VAE ($\beta = 1$), it fails completely. The reason can be traced back to the loss function given in Eq. (4), where the two terms try to match the output distribution $p_\theta(x|z)$ with the initial data associated with corresponding z and at the same time match the latent distribution $q_\phi(z|x)$ with the prior distribution $p(z)$, respectively. There is a subtle balance between them, which is controlled by the magnitude of β . If β is small and the β -term is not properly optimized, $q_\phi(z|x)$ may strongly deviate from the latent distribution and cannot be used to generate correct samples. One the other hand, if β is too large so that the first term (likelihood) is bad, the decoder may not be well trained and thus fail to reconstruct the input samples. A proper choice of β is therefore required to balance both and produce the best data generation. In this sense, β plays the role of regularization to constrain the output range of encoder and decoder correspondingly.

Figure 3 plots the resulting latent representation. We see that the samples are clustered for all three phases

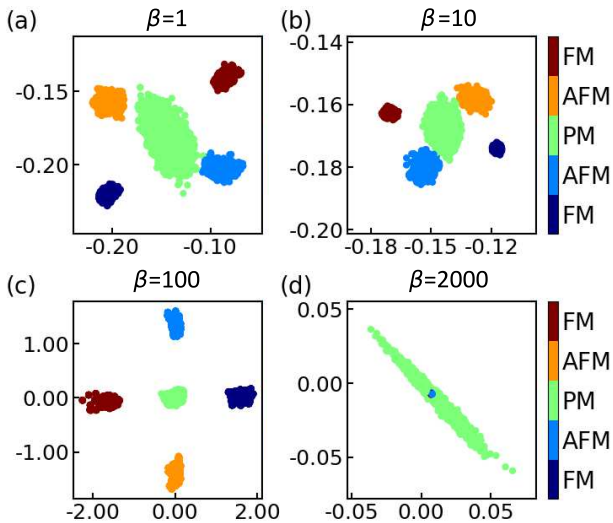


FIG. 3: Comparison of the latent representations (z) for $\beta = 1, 10, 100, 2000$. Each point represents an input sample. Only at $\beta = 100$, the disentanglement becomes axis-aligned. For $\beta = 2000$, all samples collapse together and become overlapped.

already for small $\beta = 1$. A larger β means that the deviation between $q_\phi(z|x)$ and $p(z)$ is penalized heavier. For ultra large $\beta = 2000$, all samples collapse together in the latent space and β -VAE fails to distinguish FM and AFM phases from PM. In this case, as shown in Fig. 2(d), it can only generate PM samples while ignores all features from other phases. Only for $\beta = 100$, the latent representations form a diamond shape with PM samples clustered in the center and FM and AFM samples separated into two portions on two perpendicular axes. In other words, the disentangled representations tend to be axis-aligned for FM and AFM samples. The separation and symmetric clustering on each axis in latent space reflects the Z_2 symmetry breaking of both phases. But AFM is also different from FM and contains two sublattices. The β -VAE correctly captures these properties and creates an independent parameter (the horizontal axis) to distinguish the FM and AFM samples.

The orthogonality of the latent representation ($|z_{\text{FM}}^T z_{\text{AFM}}| \approx 0$) indicates different order parameters of the FM and AFM phases. To have a more intuitive visualization of the latent space, we examine the deep learned latent representations in Fig. 4. The reconstructed data capture well the main physics of the Ising model. We see a clear consistency between disentangled representation in β -VAE and the physical order parameters for both FM and AFM phases, where the horizontal axis corresponds to magnetization for FM and the vertical axis gives the staggered magnetization for AFM. β -VAE generates AFM samples with sublattices depending on the sign of the relevant latent variable.

The latent space shows certain isometry property of

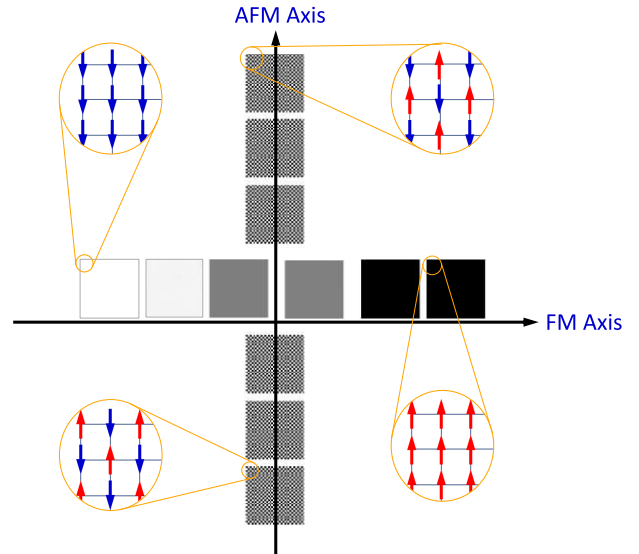


FIG. 4: Visualization of deep representations learned by β -VAE for $\beta = 100$. Each axis represents a latent variable that is seen to capture a physical order parameter. The horizontal and vertical axes correspond to the FM and AFM order parameters of the Ising model, respectively.

the encoder, namely, the relative distance in input space is protected. To see this, we may view the distribution of FM samples as a mixed distribution, $P = \frac{1}{2}P_- + \frac{1}{2}P_+$, where the subscript denotes the direction of magnetization and the coefficient reflect the Z_2 symmetry. Obviously, no similar decomposition exists in the PM phase. We may measure the dissimilarity of different phases via maximum mean discrepancy (MMD) [38] defined by

$$\text{MMD}[\mathcal{F}, P_x, P_y] \equiv \sup_{f \in \mathcal{F}} \mathbb{E}_{x \sim P_x}[f(x)] - \mathbb{E}_{y \sim P_y}[f(y)], \quad (7)$$

where P_x and P_y are the probability distribution of random variables X and Y , respectively. A closed form of MMD is usually intractable, so we approximate MMD in the scaling function space $\mathcal{F} = \{f : \mathbb{R}^N \rightarrow \mathbb{R}^N | f(x) = cx, 0 \leq c \leq 1\}$. The square of MMD then gives

$$\begin{aligned} \text{MMD}^2[\mathcal{F}, P_x, P_y] &= \sup_{0 \leq c \leq 1} c^2 (\mathbb{E}_{x \sim P_x}[x] - \mathbb{E}_{y \sim P_y}[y])^2 \\ &= (\mathbb{E}_x[x] - \mathbb{E}_y[y])^2, \end{aligned} \quad (8)$$

which is simply the square of the Euclidean norm of the difference of the first moment, namely the magnetization in Ising data. Obviously, the equality of distance between P_+ , P_- , and P_{PM} appears in both input and latent space and the isometry property is protected up to a scaling factor. The isometry property of probability plays a crucial role in reflecting the broken symmetry of the Ising model and is not included a priori in the theoretical framework of information bottleneck principle. A careful study of this property may lead to novel understanding of representation learning.

IV. DISCUSSION

How can disentangled representations consist with physical order parameters and exhibit real physical interpretation? To see this, we show that the decoder of β -VAE with Bernoulli likelihood function corresponds to solving a mean-field Hamiltonian at fixed temperature with local effective fields determined by optimization.

Given any raw data point x as a vectorized spin configuration $(\sigma_1, \dots, \sigma_{L \times L})$ for the Ising model on a square lattice, the likelihood function corresponding to the Bernoulli decoder assumes that x satisfies

$$p_\theta(x|z) = \prod_{k=1}^{L \times L} m_k^{\sigma_k} (1 - m_k)^{1 - \sigma_k}, \quad (9)$$

where $\{m_k\}$ are Bernoulli parameters as well as the output of the decoder. This can be rewritten as

$$p_\theta(x|z) = \frac{\exp(\sum_k h_k \sigma_k)}{\prod_k (1 + e^{h_k})}, \quad (10)$$

with $h_k = \log \frac{m_k}{1 - m_k}$ or $m_k = \frac{1}{1 + e^{-h_k}}$. This formula corresponds exactly to a mean-field Hamiltonian of the data and its partition function:

$$H = - \sum_k h_k \sigma_k, \quad Z = \text{Tr} e^{-H} = \prod_k (1 + e^{h_k}), \quad (11)$$

where the parameters $\{h_k\}$ play the role of local effective fields on the lattice and are determined by the decoder neural network and latent variable z . Furthermore, from the functional relation between h_k and m_k , we can see that the sigmoid activation function $\sigma : \mathbb{R} \rightarrow \mathbb{R}$, $x \rightarrow 1/(1 + e^{-x})$ in the last layer simply means that the decoder neural network is learning the local effective field $\{h_k\}$ in the last layer and then uses the activation to give the Bernoulli parameters $\{m_k\}$. Therefore, activation is equivalent to solving the Hamiltonian (11), albeit at a fixed temperature $T = 1$.

The role of β may then be understood if we rewrite the optimization of the loss function in a stepwise manner. For fixed p_θ , the optimal condition $\delta \mathcal{L} / \delta q_\phi|_{p_\theta} = 0$ yields the relation

$$q_\phi(z|x) = \frac{p(z)p_\theta(x|z)^{1/\beta}}{Z_{\theta,x}}, \quad (12)$$

where $Z_{\theta,x} = \int dz p(z) p_\theta(x|z)^{1/\beta}$ is the normalization factor. Putting this equation back to the loss function, we find $\mathcal{L} = -\beta \langle \ln Z_{\theta,x} \rangle_x$, which is a function of p_θ solely, while Z may be viewed as a partition function of latent variables. We immediately see a connection between statistical physics and β -VAE. In practice, we find that the encoder always converges faster than the decoder. This provides an empirical support to Eq. (12). In this sense, β -VAE might be viewed as a Stackelberg game [46], with the encoder being the follower and the decoder the leader.

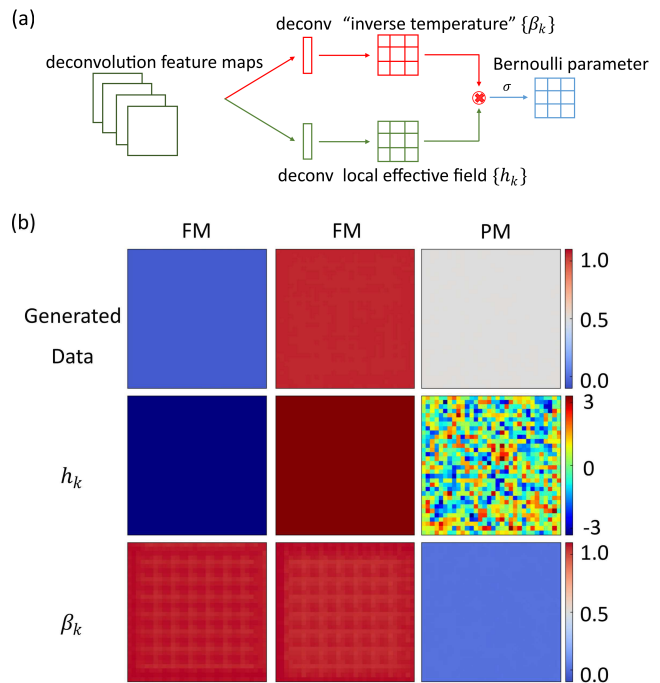


FIG. 5: (a) Illustration of the β^2 -VAE architecture, with both the “temperature branch” β_k and the original branch learning a local effective field h_k . The symbol \otimes denotes element-wise matrix multiplication. The added branch enables the model to generate samples with thermal fluctuations. (b) Comparison of generated samples for FM and PM phases and their local effective field h_k and “inverse temperature” β_k learned by β^2 -VAE for $\beta = 100$ with the constraint $0 < \beta_k < 1$.

The above formula motivates an analogy between “temperature” and β . Namely, the hyperparameter β acts as a rescaling factor of the energy and a proper choice of β enables us to ignore the fluctuations within each phase. As a result, similar samples may cluster in the latent space as demonstrated in Fig. 3. However, if β is too large, it will enforce the decoder to ignore all fluctuations and thus fail to distinguish samples of different phases in latent space. Along this line of thought and looking back on Eq. (11), one may immediately realize that the equation lacks a temperature scale so that generation via solving the Hamiltonian with sigmoid activation function contains no thermal fluctuations. This greatly limits the expressive power of β -VAE and motivates us to explore a physics-informed extension by adding an additional “temperature” branch in the loss function Eq. (4). As illustrated in Fig. 5(a), we have two separate branches to learn the local inverse temperature β_k and the local effective field h_k , respectively, and the extended algorithm parameterizes the Bernoulli distribution in a compositional way. The temperature branch can also be viewed as a special case of attention mechanism [47–49]. We name this novel algorithm as β^2 -VAE since β is also a standard usage of statistical physics for the true inverse

temperature. It has a partition function of the form,

$$\tilde{Z} = \prod_{k=1}^n (1 + e^{\beta_k h_k}), \quad (13)$$

where β_k and h_k are determined by decoder neural network. The additional β_k branch plays a similar role as the hyperparameter β in β -VAE. Combining Eq. (12) and Fig. (5), it is straightforward to view the original hyperparameter β in β -VAE as the prior global “temperature” that indicates the fluctuations of the data distribution, while the extra β_k as an adapted reweighed term to enable the decoder to determine a local temperature on each lattice site in order for a more flexible approximation of the data partition function.

To test this idea, we have performed one-phase learning by means of β^2 -VAE by training it with samples from each phase alone. Figure 5(b) shows the generated samples, learned local effective fields h_k , and local “inverse temperatures” β_k . For simplicity, β_k is valued in (0, 1) to reweigh the “global temperature” β . The generated data (first row) confirm the power of reproducing correct samples within β^2 -VAE. Given a generated sample, the corresponding local effective fields h_k (second row) successfully discover the spontaneous magnetization in the FM phase and disorder in the PM phase. Furthermore, we find a larger β_k (low temperature) in FM and a smaller β_k (high temperature) in PM, in good agreement with physical intuition. We thus conclude that the temperature branch can indeed reflect the magnitude of thermal fluctuations in the data.

V. CONCLUSION

We have studied disentangled low-dimensional representations for the Ising model using the information bottleneck method. Compared to traditional variational autoencoder, β -VAE can generate samples of appropriate physical properties with proper hyperparameter setting. The latent representation can become axis-aligned and reveal certain isometry property of the encoder. Our results confirm the consistency between learned disentangled low-dimensional representations and FM/AFM order parameters for the Ising model. This is understood by the analogy between the widely-used Bernoulli decoder with sigmoid activation function and the learning of a mean-field Hamiltonian, with the hyperparameter β reflecting a global temperature in the data. Based on this interpretation, we further notice that traditional decoder structure is unable to represent thermal fluctuations. This motivates us to propose a novel physics-informed algorithm β^2 -VAE with an extra reweighing branch of the decoder to detect fluctuations. We note that the choice of the decoder depends closely on the property of the data. For other models with non-binary

variables, the Bernoulli decoder cannot be used and the above conclusions need to be reexamined. Nevertheless, we do not expect any fundamental differences, and our approach may also be extended to more complex models.

ACKNOWLEDGEMENTS

This work was supported by the National Natural Science Foundation of China (NSFC Grant No. 11974397, No. 11774401), the National Key R&D Program of MOST of China (Grant No. 2017YFA0303103), and the Strategic Priority Research Program of the Chinese Academy of Sciences (Grant No. XDB33010100).

APPENDIX

Standard CNN architecture has been used for both β -VAE and β^2 -VAE as listed in Table I and Table II, respectively. Both the encoder and decoder contain four layers, but β^2 -VAE has two branches in the last layer. All α in Leaky-RELU (lReLU) are set to 0.2 and the batch size is set to 128. BN stands for batch normalization [50]. We have used the Adam optimizer with learning rate equal to 0.001, $\beta_1 = 0.5$, and $\beta_2 = 0.999$.

TABLE I: Neural network architecture for β -VAE.

Encoder network
Input gray image $x \in \mathbb{R}^{32 \times 32 \times 1}$
Conv2d, BN, $4 \times 4 \times 64$, stride=2, padding=SAME, lReLU
Conv2d, BN, $4 \times 4 \times 128$, stride=2, padding=SAME, lReLU
FC, BN, 1024 lReLU
FC, 2, linear; FC, 2, softplus
Decoder network
Input $z \in \mathbb{R}^2$
FC, BN, 1024, ReLU
FC, BN, 8×1024 , ReLU
Deconv2d, BN, $4 \times 4 \times 64$, stride=2, padding=SAME, ReLU
Deconv2d, $4 \times 4 \times 1$, stride=2, padding=SAME, sigmoid

* yifeng@iphy.ac.cn

- [1] K. He, X. Zhang, S. Ren, and J. Sun, “Deep residual learning for image recognition,” in *2016 IEEE Conference on Computer Vision and Pattern Recognition (CVPR)*, 2016.
- [2] A. Krizhevsky, I. Sutskever, and G. E. Hinton, “Imagenet classification with deep convolutional neural networks,” in *Advances in Neural Information Processing Systems*, 2012.

TABLE II: Neural network architecture for β^2 -VAE.

Encoder network
Input gray image $x \in \mathbb{R}^{32 \times 32 \times 1}$
Conv2d, BN, $4 \times 4 \times 64$, stride=2, padding=SAME, lReLU
Conv2d, BN, $4 \times 4 \times 128$, stride=2, padding=SAME, lReLU
FC, BN, 1024 lReLU
FC, 2, linear; FC, 2, softplus
Decoder network
Input $z \in \mathbb{R}^2$
FC, BN, 1024, ReLU
FC, BN, 8×1024 , ReLU
Deconv2d, BN, $4 \times 4 \times 64$, stride=2, padding=SAME, ReLU
Deconv2d, $4 \times 4 \times 1$, stride=2, padding=SAME, sigmoid ^a
Deconv2d, $4 \times 4 \times 1$, stride=2, padding=SAME, Linear sigmoid

^aBlank space indicates two branches in the same layer.

- [3] K. He, X. Zhang, S. Ren, and J. Sun, "Identity mappings in deep residual networks," in *European Conference on Computer Vision*, 2016.
- [4] V. Mnih, K. Kavukcuoglu, D. Silver, A. Graves, I. Antonoglou, D. Wierstra, and M. Riedmiller, "Playing atari with deep reinforcement learning," in *NIPS Deep Learning Workshop*, 2013.
- [5] J. Schrittwieser, I. Antonoglou, T. Hubert, K. Simonyan, L. Sifre, S. Schmitt, A. Guez, E. Lockhart, D. Hassabis, T. Graepel, T. P. Lillicrap, and D. Silver, "Mastering atari, go, chess and shogi by planning with a learned model," *ArXiv preprint arXiv:1911.08265*, 2019.
- [6] O. Vinyals, I. Babuschkin, W. M. Czarnecki, M. Mathieu, P. Georgiev, J. Oh, D. Horgan, M. Kroiss, I. Danihelka, A. Huang, L. Sifre, T. Cai, J. P. Agapiou, M. Jaderberg, A. S. Vechnevets, R. Leblond, T. Pohlen, V. Dalibard, D. Budden, Y. Sulsky, J. Molloy, T. L. Paine, C. Gulcehre, Z. Wang, T. Pfaff, Y. Wu, R. Ring, D. Yogatama, D. Wünsch, K. Mckinney, O. Smith, T. Schaul, T. Lillicrap, K. Kavukcuoglu, D. Hassabis, C. Apps, and D. Silver, "Grandmaster level in Starcraft II using multi-agent reinforcement learning," *Nature* **575**, 350 (2019).
- [7] F. Locatello, S. Bauer, M. Lucic, G. Raetsch, S. Gelly, B. Schölkopf, and O. Bachem, "Challenging common assumptions in the unsupervised learning of disentangled representations," in *Proceedings of the 36th International Conference on Machine Learning*, 2019.
- [8] Y. Bengio, A. Courville, and P. Vincent, "Representation learning: A review and new perspectives," *IEEE Transactions on Pattern Analysis and Machine Intelligence*, **35**, 179 (2013).
- [9] H. Kim and A. Mnih, "Disentangling by factorising," in *Proceedings of the 35th International Conference on Machine Learning*, 2018.
- [10] Y. Bengio, Y. Lecun, and G. Hinton, "Deep learning," *Nature* **521**, 436 (2015).
- [11] C. P. Burgess, I. Higgins, A. Pal, L. Matthey, N. Watters, G. Desjardins, and A. Lerchner, "Understanding disentangling in beta-vae," in *Workshop on Learning Disentangled Representations at the 31st Conference on Neural Information Processing Systems*, 2017.
- [12] I. Goodfellow, J. Pouget-Abadie, M. Mirza, B. Xu, D. Warde-Farley, S. Ozair, A. Courville, and Y. Bengio, "Generative adversarial nets," in *Advances in Neural Information Processing Systems*, 2014.
- [13] X. Chen, Y. Duan, R. Houthoofd, J. Schulman, I. Sutskever, and P. Abbeel, "InfoGAN: Interpretable representation learning by information maximizing generative adversarial nets," in *Advances in Neural Information Processing Systems*, 2016.
- [14] D. P. Kingma and M. Welling, "Autoencoding variational bayes," in *Proceedings of the International Conference on Learning Representations*, 2014.
- [15] D. J. Rezende, S. Mohamed, and D. Wierstra, "Stochastic backpropagation and approximate inference in deep generative models," in *Proceedings of the 31th International Conference on Machine Learning*, 2014.
- [16] P. Smolensky, *Information processing in dynamical systems: Foundations of harmony theory*. Cambridge: MIT Press, 1986.
- [17] M. H. Amin, E. Andriyash, J. Rolfe, B. Kulchytskyy, and R. Melko, "Quantum Boltzmann machine," *Phys. Rev. X*, **8**, 021050 (2018).
- [18] M. Koch-Janusz and Z. Ringel, "Mutual information, neural networks and the renormalization group," *Nature Physics*, **14**, 578 (2018).
- [19] A. Nagy and V. Savona, "Variational quantum Monte Carlo method with a neural-network ansatz for open quantum systems," *Phys. Rev. Lett.* **122**, 250501 (2019).
- [20] M. J. Hartmann and G. Carleo, "Neural-network approach to dissipative quantum many-body dynamics," *Phys. Rev. Lett.* **122**, 250502 (2019).
- [21] F. Vicentini, A. Biella, N. Regnault, and C. Ciuti, "Variational neural-network ansatz for steady states in open quantum systems," *Phys. Rev. Lett.* **122**, 250503 (2019).
- [22] N. Yoshioka and R. Hamazaki, "Constructing neural stationary states for open quantum many-body systems," *Phys. Rev. B* **99**, 214306 (2019).
- [23] G. Torlai and R. G. Melko, "Learning thermodynamics with Boltzmann machines," *Phys. Rev. B* **94**, 165134 (2016).
- [24] G. Torlai, G. Mazzola, J. Carrasquilla, M. Troyer, R. Melko, and G. Carleo, "Neural-network quantum state tomography," *Nature Physics*, **14**, 447 (2018).
- [25] G. Torlai and R. G. Melko, "Latent space purification via neural density operators," *Phys. Rev. Lett.* **120**, 240503 (2018).
- [26] G. Carleo and M. Troyer, "Solving the quantum many-body problem with artificial neural networks," *Science* **355**, 602 (2017).
- [27] A. Morningstar and R. G. Melko, "Deep learning the Ising model near criticality," *Journal of Machine Learning Research* **18**, 1 (2018).
- [28] F. D'Angelo and L. Böttcher, "Learning the Ising model with generative neural networks," *ArXiv preprint: arXiv:2001.05361*, 2020.
- [29] S. Efthymiou, M. J. S. Beach, and R. G. Melko, "Super-resolving the Ising model with convolutional neural networks," *Phys. Rev. B* **99**, 075113 (2019).
- [30] B. Schölkopf, A. Smola, and K.-R. Müller, "Kernel principal component analysis," in *Artificial Neural Networks — ICANN'97*, 1997.
- [31] L. Wang, "Discovering phase transitions with unsuper-

- vised learning,” *Phys. Rev. B*, **94**, 195105 (2016).
- [32] S.-H. Li and L. Wang, “Neural network renormalization group,” *Phys. Rev. Lett.* **121**, 260601 (2018).
- [33] S. Iso, S. Shiba, and S. Yokoo, “Scale-invariant feature extraction of neural network and renormalization group flow,” *Phys. Rev. E* **97**, 053304 (2018).
- [34] D. Kim and D.-H. Kim, “Smallest neural network to learn the Ising criticality,” *Phys. Rev. E* **98**, 022138 (2018).
- [35] X. Gao, Z. Zhang, and L.-M. Duan, “A quantum machine learning algorithm based on generative models,” *Science Advances*, **4**, 2018.
- [36] S. Lloyd and C. Weedbrook, “Quantum generative adversarial learning,” *Phys. Rev. Lett.* **121**, 040502 (2018).
- [37] C. Zoufal, A. Lucchi, and S. Woerner, “Quantum Generative Adversarial Networks for learning and loading random distributions,” *npj Quantum Information* **5**, 103 (2019).
- [38] A. Gretton, K. M. Borgwardt, M. J. Rasch, B. Schölkopf, and A. Smola, “A kernel two-sample test,” *Journal of Machine Learning Research* **13**, 723 (2012).
- [39] N. Tishby, F. Pereira, C., and W. Bialek, “The information bottleneck method,” in *Proceedings of the 37-th Annual Allerton Conference on Communication, Control and Computing*, 1999.
- [40] R. Shwartz-Ziv and N. Tishby, “Opening the black box of deep neural networks via information,” *arXiv preprint arXiv:1703.00810*, 2017.
- [41] A. A. Alemi, I. Fischer, J. Dillon, V., and K. Murphy, “Deep variational information bottleneck,” in *Proceedings of the International Conference on Learning Representations*, 2017.
- [42] L. Onsager, “Crystal statistics. i. a two-dimensional model with an order-disorder transition,” *Phys. Rev.* **65**, 117 (1944).
- [43] M. Abadi, P. Barham, J. Chen, Z. Chen, A. Davis, J. Dean, M. Devin, S. Ghemawat, G. Irving, M. Isard, M. Kudlur, J. Levenberg, R. Monga, S. Moore, D. G. Murray, B. Steiner, P. Tucker, V. Vasudevan, P. Warden, M. Wicke, Y. Yu, and X. Zheng, “Tensorflow: A system for large-scale machine learning,” in *12th USENIX Symposium on Operating Systems Design and Implementation (OSDI 16)*, (Savannah, GA), 265 (2016).
- [44] D. P. Kingma and J. Ba, “Adam: A method for stochastic optimization,” in *Proceedings of the International Conference on Learning Representations*, 2015.
- [45] M. D. Hoffman, M. J. Johnson, and G. Brain, “ELBO surgery: yet another way to carve up the variational evidence lower bound,” in *Workshop in Advances in Approximate Bayesian Inference, NIPS*, 2016.
- [46] J. González-Díaz, I. García-Jurado, G. Fiestras-Janeiro, *An Introductory Course on Mathematical Game Theory*, American Math. Society (2010).
- [47] A. Vaswani, N. Shazeer, N. Parmar, J. Uszkoreit, L. Jones, A. N. Gomez, L. u. Kaiser, and I. Polosukhin, “Attention is all you need,” in *Advances in Neural Information Processing Systems*, 2017.
- [48] A. Parikh, O. Täckström, D. Das, and J. Uszkoreit, “A decomposable attention model for natural language inference,” in *Proceedings of the 2016 Conference on Empirical Methods in Natural Language Processing*, 2016.
- [49] J. Cheng, L. Dong, and M. Lapata, “Long short-term memory-networks for machine reading,” in *Proceedings of the 2016 Conference on Empirical Methods in Natural Language Processing*, 2016.
- [50] S. Ioffe and C. Szegedy, “Batch normalization: Accelerating deep network training by reducing internal covariate shift,” in *Proceedings of the 32nd International Conference on Machine Learning*, 2015.